Volume Graphics (2005)
E. Gröller, I. Fujishiro (Editors)

A Simplified Model for Inhomogeneous Subsurface Scattering

Richard Sharp† and Raghu Machiraju‡

The Ohio State University

Abstract

In recent years there has been considerable interest in modeling realistic subsurface light scattering in materials such as marble, human skin, or clouds. Many of these models provide a solution for the transport equation in a homogeneous or layered scattering media. The model we present here exploits a diffusion mechanism to provide a simpler solution to the transport equation. Treating light flux as current we can use circuit analysis techniques and linear systems to solve directly for the steady state transport equation and ignore the transient values. Thus our model can simulate light transport in heterogeneous materials and complex geometry.

Categories and Subject Descriptors (according to ACM CCS): I.3.3 [Computing Methodologies]: Computer GraphicsPicture/Image Generation; I.3.7 [Computing Methodologies]: Computer GraphicsThree-Dimensional Graphics and Realism

1. Introduction

Subsurface scattering and substrate rendering is arguably one of the most challenging aspects of realistic image synthesis today. This effect is what makes organic material, such as skin, look soft [JMLH01]. Similarly, substrate effects allows for the rendering of patinas and weathering [DH96]. Photorealism will certainly require that scattering and substrate effects be included for convincing visuals.

Previous research in this area has yielded various models of light transport, each suited for modeling scattering and substrate transport in different types of materials [BR98, Bli82, DH96, HK93, JMLH01, Max94, Sta95].

Very realistic looking images have been obtained through these models. Unfortunately, many of them have limitations such as restrictions to simple geometries [BR98, Bli82, Max94], homogeneous materials [JMLH01, Max94, Bli82] or are limited to one dimensional transport theory or BRDFs [BR98, Bli82, DH96, HK93, KPHE02, REHL03].

It should be noted that the methods reported previously do not allow one to model and conceive virtual and realistic materials to achieve a diversity of light scattering effects. Consider the task of rendering organic material such as a tomato (see Figure 7). One can perhaps assume homogeneity and select a suitable value for the scattering and extinction coefficients for the model proposed in [JMLH01]. However, a tomato is hardly homogeneous. It is composed of the pericarp, which is a highly scattering vascular tissue; the exocarp, thin outer skin; placental tissue, a gelatinous membrane surrounding the seeds with low absorption and scattering properties; and the seeds, which are opaque. Furthermore, these tissues are not layered in any regular or periodic fashion, hence a continuous solution cannot be derived.

In this paper we realize a transport model that incorporates material modeling and addresses the issues raised above. The salient features of our transport model are listed below:

- Light transport in the material is conservative. In other words all light energy is accounted for by either generation from a source, absorption as heat, or scattering into or out of the system.
- The medium is highly scattering (optically thick) and hence can be modeled using a diffusion approximation.
- Transients in the medium are not necessary for rendering. The only data we are often interested in is obtained from solution of the steady state.

These assumptions will naturally lead to a diffusive interpretation of the light transport. A diffusive approximation will certainly be less accurate than more realistic complete

† email: sharpr@cis.ohio-state.edu
‡ email: raghu@cis.ohio-state.edu

© The Eurographics Association 2005.

delivered by EUROGRAPHICS DIGITAL LIBRARY www.eg.org diglib.eg.org

simulations which often rely on Monte Carlo solutions of integral Equations [Cha60, Kaj86, Pra88]. It should be noted that the complete solutions are often very computationally expensive and the handling of boundary conditions can be often intractable. On the other hand, a diffusive approximations can be more accurate than heuristic methods including the Kubelka-Munk method [DH96].

Diffusion is the primary means of light propagation in a highly scattering subsurface. Thus, in the computer graphics literature diffusion has been used to model subsurface scattering [JMLH01, Sta95]. However, we employ a simpler scattering framework and show how inhomogeneity can be included. In essence we employ a restricted model of transport where flux (or light) propagates along a 3D grid of cells. *Although this may seem restrictive it should be noted that in the limiting case our cell transport diffusion model will model the complete diffusion process and hence subsurface scattering in its entirety.* While it is possible to bias a phase function in diffusion to forward or backward scatter our model prefers neither direction.

Diffusion methods can be realized from a system of partial differential equations. However, other more intuitive methods exist. The steady state behavior of an impedance network (an electrical circuit) could also provide a diffusive realization of light transport. In essence, we create an optical network. We consider the dual of light propagated though the scattering media as current or "flux" through the electric circuit. Voltage sources model the initial boundary conditions of the light incident on the material, grounding elements inside cells simulate absorption and intercellular impedances model the directions and relative amount of flux that can be scattered from and into a cell.

Furthermore, modeling subsurface scattering as an electric circuit provides additional benefits that have not, to our knowledge, been previously addressed together in a scattering model to date:

- Inhomogeneous materials are easily modeled. As an example later in this paper we create an inhomogeneous light scattering model for a tomato and a human foot based on Magnetic Resonance (MR) data. The scalar field can be used as a reference to a transfer function to map MR intensities to scattering properties[†].
- User defined inhomogeneous substrates can be easily built. Once the scattering properties of a particular material have been studied and converted to its dual in an electric circuit, it can be used like a building block in combination with other blocks to generate a new material.
- Some models that exist today must rely on thin materials, or only allow connections in specific directions. No restrictions need to be made on the geometry of our model. Connections can exist in any direction and across cells if necessary.
- Use of an electric circuit provides us with many fast and robust numerical solution techniques.
- Rendering now is post-processing activity after a steady state solution is obtained, thus simpler algorithms than photon mapping can be used for rendering.

[†] Although we describe a regular subdivision it should be noted that our technique can be applied to any subdivision of space.

1.1. Paper Overview

The rest of our paper is as follows. First in Section 2 we discuss previous works including different subsurface light scattering models. Next in Section 3 we provide an introduction to our cell transport theory and tie our circuit model with previous models by showing how voltage can be derived from irradiance. Following this in Section 4 we describe the computational methods we employed. Finally in Section 5 we show the complex scattering behavior our model can simulate by varying the composition of the scattering substrate. Furthermore we show how MRI density values can be used to set constraints on the optical network. We present our final results in Section 7.

2. Previous Work

S. Chandrasekhar first presented the equation of transport in his classic work *Radiative Transfer* [Cha60] (see Equation 5). This equation essentially accounts for all radiance flowing through a surface by accounting for absorption, outscattering, inscattering and a source term. Any effort to model subsurface scattering or substrate transport of light is in reality an attempt to solve this equation. Kajiya was one of the first to use this mathematical machinery and proposed a stochastic approach of path tracing and Monte Carlo methods [Kaj86].

Blinn created the first subsurface scattering model in computer graphics. His goal was to realistically model light scattering effects caused by the rings of Saturn [Bli82]. Blinn's model uses various Henyey-Greenstein functions and physically based measurements to create probability distributions for particle scattering directions. Although the resulting model is elegant and generates impressive images, it is limited to thin surfaces of low albedo and does not account for higher order scattering events. On a similar note Kajiya and Von Herzen present the classic volume ray tracing algorithm [KV84] while Rushmeier and Torrance present a radiosity based solution for a similar scattering problem [RT87].

Baranoski and Rokne developed model similar to Blinn's for light transport in plant tissue [BR98]. However, the phase functions are more complex than that of Blinn's and are obtained from large number of physically based measurements. Once again only thin materials can be modeled.

Hanrahan and Kruger developed a bidirectional reflectance distribution function (BRDF) and a transport

© The Eurographics Association 2005.

model for subsurface scattering that is a complete solution to the total first order scattering [HK93]. Unfortunately it is limited to flat, uniformly lit, homogeneous slabs and is based on one dimensional transport theory along a ray (i.e. does not take into account scattering from neighboring areas). Higher order scattering terms can be determined through the use of a Neumann series expansion.

Jensen et al. [JMLH01] introduced a fast Monte-Carlo subsurface scattering model that combined the diffusion approximation presented by Ishimaru [Ish78] and the single order scattering BRDF from Hanrahan and Kruger. Furthermore, the authors used a dipole source to satisfy the boundary condition in Ishimaru's diffusion approximation. As a result, Jensen et al. propose the use of the bidirectional surface scattering distribution function (BSSRDF) which is like a BRDF but allows flux to exit a substrate in a different location than it entered. It should be noted that the model which uses the dipole formulation is limited to homogeneous materials only.

Jensen proposed a variant of photon mapping for highly scattering materials in [Jen01]. In this model diffuse photons are discretely traced through the substrate where at each time step a photon is either scattered, absorbed or left untouched for the next time step. The exiting diffuse light is estimated by gathering photons in the region that is to be lighted. This technique could be made to handle non-homogeneous materials, but would require variable stepsizes depending on the scattering properties of the current material the photon is being traced through. Also, during the gathering step one must account for the contribution of photons differently depending on the scattering properties of the material that that photon resides.

Max [Max94] presented an enhancement to the discrete ordinates method which accounts for multiple scattering. In this method each voxel can scatter flux into a finite number of directions entire solid angles. Max et al. [MSM*04] enhances this method by taking advantage of hardware accelerated techniques and accounting for regions in clouds with little scattering.

Jos Stam presented an implementation of multiple scattering as a diffusion processes in [Sta95]. Stam's diffusion model was also derived from Ishimaru [Ish78] but solved the diffusion process through a multi-grid finite difference scheme and a finite-element blob method. Ishimaru shows that one can use the diffusion approximation to accurately simulate light propagation through materials when scattering events are frequent. These occur in optically thick materials like skin or milk. Since we also use a diffusion approximation it should be noted that this transport model is similar to ours. However, in our model we treat light flux as potentials across neighboring voxels rather than continuous flux throughout the substrate.

Kniss et al. [KPH*03] has developed a model that uses forward scattering and volumetric light attenuation to improve the quality of volume shading. A model of this nature is useful in materials where forward scattering dominates, such as highly translucent material, clouds or even atmospheric effects [KPHE02, REHL03].

Researchers in biomedical engineering have also examined the transport of electromagnetic radiation and waves in human tissue [PH97, Pra88]. In [Pra88] a diffusion approximation, the Delta-Eddington model, was used to model light transport. Specific boundary conditions were used to model various tissue arrangements and configurations. Also, measurements were included in the model for more accurate modeling of the transport phenomena. It should be noted that circuits are often used to model light propagation in media [PH97].

Finally there has been a significant amount of work done to simulate subsurface scattering on modern graphics hardware [MKB*03, DS03] through simplifications of the scattering model or through implementation of numerical methods on the graphics processing unit.

3. Theory

To recapitulate, our transport model is realized as a steady state diffusion process and can be conceived as an electrical circuit. As a result inhomogeneous materials, complex geometries and measurements can be easily included. In essence, our approach provides a bread-board for constructing complex materials and render them expediently.

This section provides necessary justification for our model as well as an introduction to basic circuit theory which we will use to derive our linear system of equations in a later section.

3.1. Cell Transport Model

Our model assumes that the solution for light propagation through highly scattering media is the same as voltage propagation through a resistive network. This section will show how light is related to current and how the solution of a resistive network is the same as the solution to the transport equation.

3.1.1. Irradiance is Related to Voltage

Irradiance (flux per unit area) is the integration of incoming radiance over all directions, its units are W/m^2. Hence, we can write irradiance as power per unit area:

$$\frac{d\phi}{dA} = E = \frac{p}{dA}. \tag{1}$$

Likewise in circuit theory we can write power as a product of voltage and current:

© The Eurographics Association 2005.

$$p = \frac{dw}{dt} = \frac{dw}{dq} \cdot \frac{dq}{dt} = vi. \quad (2)$$

From Ohm's law we can rewrite this equation in terms of voltage only:

$$p = \frac{v^2}{R}. \quad (3)$$

Resistor R has no physical significance in our optical network other than the initial value of the voltage and hence can be chosen arbitrarily. This leads us to understand the relationship between voltage and irradiance as:

$$E \propto \frac{v^2}{dA} \Rightarrow v \propto \sqrt{E \cdot dA}. \quad (4)$$

3.1.2. Transport Equation in terms of Kirchoff Current Laws

In this section we show how the Transport Equation can be realized as a diffusion equation, and then how the diffusion equation can be realized in terms of Kirchoff Current Laws.

Ishimaru shows that single scattering and first order solutions are applicable when the volume density (ratio of the volume occupied by particles to the total volume of the media) is much less than 0.1% [Ish78] (such as Blinn's Saturn rings). The diffusion approximation gives good solutions when the density is much greater than 1% which exists in highly scattering media, such as blood [Joh70].

Intensity in a random medium can be divided into two parts, the reduced incident intensity I_{ri} and the diffuse intensity I_d. Reduced incident intensity is the part of the flux that remains after scattering and absorption. We denote it by $I_{ri}(\mathbf{r},\vec{\mathbf{s}})$ where $\mathbf{r}$ is the point at which the flux is measured and $\vec{\mathbf{s}}$ is the unit vector in which it is propagating. Its behavior satisfies the equation

$$\frac{dI_{ri}(\mathbf{r},\vec{\mathbf{s}})}{ds} = -\rho\sigma_t I_{ri}(\mathbf{r},\vec{\mathbf{s}})$$

which simply shows that the value of I_{ri} decays exponentially as we travel away from its origin where ρ is the particle density and σ_t is the extinction cross section. This behavior is similar to ray techniques used in volume rendering. (Note that terms are described in Table 1).

The diffuse intensity must satisfy the equation of transfer:

$$\frac{dI_d(\mathbf{r},\vec{\mathbf{s}})}{ds} = -\rho\sigma_t I_d(\mathbf{r},\vec{\mathbf{s}}) + \frac{\rho\sigma_t}{4\pi}\int_{4\pi} p(\vec{\mathbf{s}},\vec{\mathbf{s}}')I_d(\mathbf{r},\vec{\mathbf{s}})d\omega' + \varepsilon_{ri}(\mathbf{r},\vec{\mathbf{s}}) + \varepsilon(\mathbf{r},\vec{\mathbf{s}}). \quad (5)$$

$p(\hat{\mathbf{s}},\hat{\mathbf{s}}')$	the phase function of the angle between $\hat{\mathbf{s}}$ and $\hat{\mathbf{s}}'$.
$\bar{\mu}$	the mean cosine of the scattering angle
ρ	particle density
σ_a	absorption cross section
σ_s	scattering cross section
σ_t	extinction cross section $(\sigma_a + \sigma_s)$
σ_{tr}	transport cross section $(\sigma_s(1-\bar{\mu}) + \sigma_a)$
$I_d(\mathbf{r},\hat{\mathbf{s}})$	diffuse intensity
$I_{ri}(\mathbf{r},\hat{\mathbf{s}})$	reduced incident intensity
$\varepsilon(\mathbf{r},\hat{\mathbf{s}})$	source function
$\varepsilon_{ri}(\mathbf{r},\hat{\mathbf{s}})$	source function due to reduced incident intensity
$U_d(\mathbf{r})$	average diffuse intensity
$U_{ri}(\mathbf{r})$	average reduced intensity
κ	$(\rho\sigma_{tr})^{-1}$
α	$3\rho\sigma_a$

Table 1: *Table of terms*

In this case ε_{ri} is the reduced source term which can be calculated from the reduced intensity and ε is simply an internal source term (if one exists).

By expanding I_d into the first two terms of its Taylor's series expansion and substituting back into Equation 5 we end up with the steady state diffusion approximation (see the details of the derivation in [Ish78] pp 175-178):

$$\nabla^2 U_d(\mathbf{r}) - \kappa^2 U_d(\mathbf{r}) = -3\rho^2\sigma_s\sigma_{tr}U_{ri}(\mathbf{r}) - \frac{3}{4\pi}\rho\sigma_{tr}E(\mathbf{r}) + \frac{3}{4\pi}\nabla\cdot\int_{4\pi}\varepsilon_{ri}(\mathbf{r},\vec{\mathbf{s}})\vec{\mathbf{s}}d\omega + \frac{3}{4\pi}\nabla\cdot\int_{4\pi}\varepsilon(\mathbf{r},\vec{\mathbf{s}})\vec{\mathbf{s}}d\omega. \quad (6)$$

Where, U_d and U_{ri} are the uniform diffuse and reduced intensities respectively. By collecting the scattering terms, we write this equation in a more general form,

$$\nabla^2 u - au = \varepsilon \quad (7)$$

where

- u diffusion term
- a absorption coefficient
- ε source term.

We present Equation 7 in finite difference form. Assuming we divide our volume up into equal Cartesian cubes of width h:

© The Eurographics Association 2005.

$$\varepsilon_{ijk} = -au_{ijk} + \frac{\triangleright_x(u_{ijk}) + \triangleleft_x(u_{ijk}) + \triangleright_y(u_{ijk}) + \triangleleft_y(u_{ijk}) + \triangleright_z(u_{ijk}) + \triangleleft_z(u_{ijk})}{h^2} \tag{8}$$

Where the forward and backward different operators $\triangleright_x$ and $\triangleleft_x$ are defined as

$$\begin{aligned} \triangleright_x(u_{i,j,k}) &= u_{i+1,j,k} - u_{i,j,k} \\ \triangleleft_x(u_{i,j,k}) &= u_{i-1,j,k} - u_{i,j,k}. \end{aligned}$$

As shown previously it is possible to represent irradiance in terms of voltage or current, knowing this we treat $u_{i,j,k}$ as a current flowing through the center of a finite volume centered at position (i,j,k). To model the potential for current to spread to neighboring finite elements we connect the nodes through discrete resistors whose values represent the likelihood of current to pass through the space between the two points, much like a phase function. We represent absorption as a grounded resistor attached to a node, and the source term as a DC voltage source attached through a resistor to the node.

Thus we can rewrite Equation 8 as a current equation in terms of node voltages and resistances for every cell (i,j,k):

$$\frac{V_{i,j,k}}{R_{g_{i,j,k}}} = -\frac{\Delta_V V s_{i,j,k}}{R_{s_{i,j,k}}} + \frac{1}{h^2}\left(\frac{\Delta_V V_{i+1,j,k}}{R_{i+,j,k}} + \frac{\Delta_V V_{i-1,j,k}}{R_{i-,j,k}} + \frac{\Delta_V V_{i,j+1,k}}{R_{i,j+,k}} + \frac{\Delta_V V_{i,j-1,k}}{R_{i,j-,k}} + \frac{\Delta_V V_{i,j,k+1}}{R_{i,j,k+}} + \frac{\Delta_V V_{i,j,k-1}}{R_{i,j,k-}}\right) \tag{9}$$

where $\Delta_V v \equiv v - V_{i,j,k}$ and $R_{i+,j,k}$ is defined as the resistor connecting nodes (i,j,k) and $(i+1,j,k)$, similarly, $R_{i-,j,k}$ indicates the resistor connecting nodes (i,j,k) and $(i-1,j,k)$ and so on. These resistor values represent preferred scattering directions in the material, where the lower the value, the higher the scatter. Note that these resistors are generalization of the extinction and scattering coefficient.

4. Solution Methods

This section will discuss various data structures and algorithms we used to implement our transport impedance network.

4.1. Storage

As presented earlier, Equation 9 is defined for every cell. Hence an impedance grid of a reasonable size can result in a fairly large linear system.

Fortunately, our model limits flux transport to only neighboring cells so that each equation will be dependent on a relatively small number of other equations. The result is a very sparse linear system of equations which allows us to use sparse matrix storage techniques.

To store our linear system we use the row-indexed sparse matrix storage mode presented in [PTVF92]. This technique requires approximately $2d + 2n$ space to store n non-zero elements in a matrix of size $d \times d$.

4.2. Solving the system

Once we establish our linear system of equations we must solve a system of the form

$$Ax = b. \tag{10}$$

In our implementation we used an implementation of Biconjugate Gradient from the IML++ library [BBC*94]. Biconjugate Gradient solves a series of recurrences which center around multiplying a vector by A and A^T during each iteration of the numerical method.

Fortunately the use of row-indexed storage data structure allows these multiplications to be done in $O(n)$ where n is the number of non-zero elements in A.

5. Circuit Response to Stimulus

We employ a discrete 15×15 grid to compare our model and the diffusion approximation given by the Jensen et al. model [JMLH01]. The optical properties that were chosen were within range of the "Wholemilk" data recorded in the same paper.

It may not seem practical or realistic to simulate a subsurface scattering model on a two dimensional grid; however, the Jensen et al. model doesn't really consider the transport phenomena beneath the surface. Our BSSRDF is described through the choice of the optical properties of the medium.

We provide the two dimensional grid with a step input shown in Figure 1. In the model presented in [JMLH01] this corresponds to a unit level of irradiance incident on the surface, while in our model it corresponds to setting the middle group of cells' source voltage to approximately 1 volt.

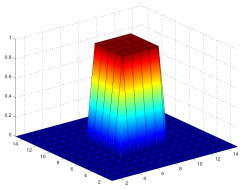

Figure 1: *Initial source values.*

The response from the [JMLH01] model and our impedance network is shown in Figure 2 which are quite similar.

© The Eurographics Association 2005.

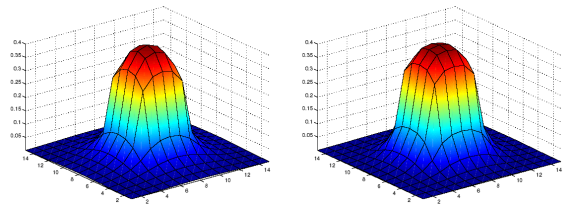

Figure 2: *Response of Jensen et al. [JMLH01] model with* $\sigma_a = 0.0041$ *and* $\sigma_s' = 2.6$ *(left) vs. Response of our model with 1.18V step input and all resistors set to 1k*Ω *(right).*

5.1. Inhomogeneous material

We ran additional experiments on inhomogeneous data which our model is able to handle without difficulty. One example is a material that has a vee-like impedance grid, where peaks occur on opposite corners and a line of low impedance strides diagonally between the opposing corners. The response in Figure 3 also has a local valley where the response peaked in earlier examples (remember that low impedance values for absorption correspond to high absorption).

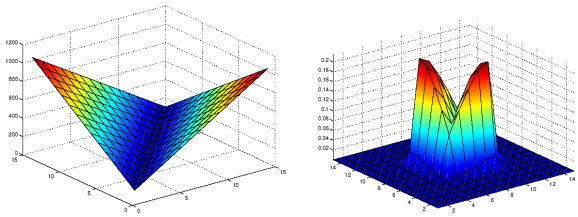

Figure 3: *Vee-like impedance (left) vs. response (right).*

Our final inhomogeneous example sets impedance values based on MRI scalar data. We can extract a desired isosurface and use that to apply the initial voltage (intensity) source values. Figure 4 shows the original slice and the solved intensity values from it.

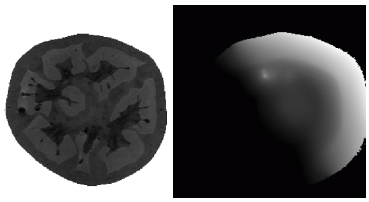

Figure 4: *Slice of MRI tomato data and the solved intensity distribution throughout the material.*

To set the internal impedance values we can use transfer functions which maps tissue types to impedance values. This is similar to efforts in volume rendering [KD98]. For example the locule tissue has low scattering properties while the endocarp is highly scattering. Based on the histogram we generated an arbitrary transfer function for absorption resistors by fitting a polynomial to points loosely based on the authors' observations on scattering properties of the tomato tissue. Figure 5 shows the histogram and a typical transfer function where high impedances refer to low absorption rates.

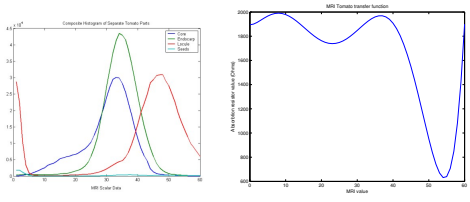

Figure 5: *Histogram of tomato tissue values (left) and the resulting transfer function (right).*

We have designed our model such that it is logical to map MRI data to the absorption and scattering properties of the tissue in question. In general, to render an object, we first extract the isosurface from the MRI data, then construct an impedance grid based on the values internal to the isosurface. The impedance values cannot be directly derived from the MRI data, but gives information about the tissue types in the slice. Therefore we pick impedance values for the circuit based on a transfer function from MRI scalar data to the known scattering properties of the tissues in the dataset.

6. Rendering

Our general rendering algorithm is as follows:

1. Extract an isosurface from the MRI dataset.
2. Build a grid to fit inside the isosurface.
3. Set the impedance values on the internal grid based on a mapping from the MRI scalar data with the transfer function.
4. Initialize the source voltages by sampling the irradiance across the boundary surface exposed in each cell as described in Equation 4.
5. Solve for node voltages.
6. Render the image by treating the solved grid as a 3D luminare and projecting it onto the surface of the 3D model much like projecting a 3D texture as a light map which illuminates the scene. The node voltages are proportional to the intensity values exiting the material.

It should be noted that although we use MRI data to derive impedance values in our model, if the material scattering properties are known they can be used directly.

7. Results

Figures 7 and 6 show the difference between scattering and no scattering from isosurfaces of a tomato and a human foot

© The Eurographics Association 2005.

respectively, which use impedance values based on the MRI scalar data. Figure 8 is particularly interesting since it compares the difference between using constant impedance values and impedance values derived directly from the MRI data.

Most of the linear systems converged in around 2 minutes on a Pentium VI 2.4 GHz machine with 2GB of RAM. Since biconjugate gradient is an iterative technique it was unnecessary to iterate the entire N cycles, where N is the number of grid elements, to achieve good results. In fact on the foot dataset which has $128 \times 128 \times 64$ elements, 14 to 30 iterations were sufficient to generate acceptable visual results. The rendering step only involves projecting a 3D texture onto a 2D surface, actual rendering times were on the order of seconds.

8. Conclusions

The use of an impedance network provides advantages not available from other techniques that model subsurface scattering and substrate transport. These advantages include the ability to easily model homogeneous materials, build user defined impedance networks and provide a model which can be solved easily using numerical linear algebra techniques. We also feel that our model is interesting since it is a realization of a unification of several otherwise unrelated mathematical models. Despite the advantages of using an impedance network to realize subsurface scattering there are still some kinds of materials our model cannot handle as well.

- Transparent materials - Since we are modeling subsurface scattering as a diffusion process, transparent materials would not render correctly in our model.
- Thin materials - While our model can handle thin materials, there are less computationally complex models which are better suited for this task.

For future work we will examine the use of active components to include anisotropic scattering effects and create more complex data to impedance transfer functions for more complex results. We will also consider non-regular decomposition of the space and make use of finite element techniques.

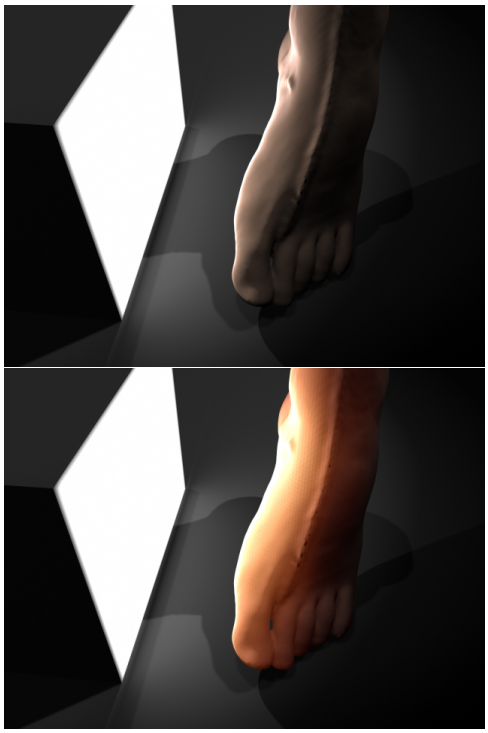

Figure 6: *Side lit foot with no scattering vs. scattering. (See color plate for full size).*

References

[BBC*94] BARRETT R., BERRY M., CHAN T. F., DEMMEL J., DONATO J., DONGARRA J., EIJKHOUT V., POZO R., ROMINE C., DER VORST H. V.: *Templates for the Solution of Linear Systems: Building Blocks for Iterative Methods, 2nd Edition*. SIAM, Philadelphia, PA, 1994. 5

[Bli82] BLINN J. F.: Light reflection functions for simulation of clouds and dusty surfaces. *Computer Graphics* (July 1982), 21–29. 1, 2

[BR98] BARANOSKI G., ROKNE J.: A simplified model for light interaction with plant tissue. In *Eighth International Conference on Computer Graphics and Visualization - GraphiCon'98* (September 1998), pp. 154–161. 1, 2

[Cha60] CHANDRASEKHAR S.: *Radiative Transfer*. Dover Publications, Inc., 1960. 2

[DH96] DORSEY J., HANRAHAN P.: Modeling and rendering of metallic patinas. In *Proceedings of the 23rd annual conference on Computer graphics and interactive techniques* (1996), ACM Press, pp. 387–396. 1, 2

[DS03] DACHSBACHER C., STAMMINGER M.: Translucent shadow maps. In *Proceedings of the 14th Eurographics workshop on Rendering* (2003), Eurographics Association, pp. 197–201. 3

[HK93] HANRAHAN P., KRUEGER W.: Reflection from layered surfaces due to subsurface scattering. In *Proceedings of the 20th annual conference on Computer graphics and interactive techniques* (1993), ACM Press, pp. 165–174. 1, 3

[Ish78] ISHIMARU A.: *Wave Propagation and Scattering in Random Media*. Academic Press, New York, 1978. 3, 4

© The Eurographics Association 2005.

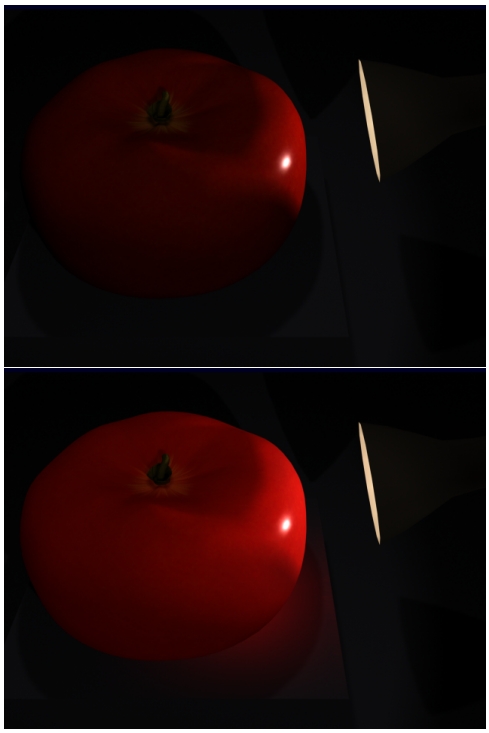

Figure 7: *Tomato with no scattering vs. tomato with scattering impedance values based on MRI data. In this case inhomogeneous scattering properties do not affect the visual appearance significantly. (See color plate for full size).*

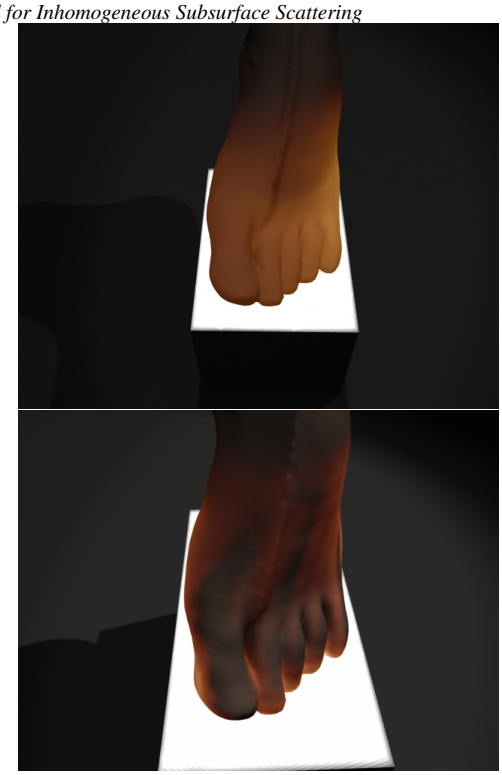

Figure 8: *Bottom lit foot with scattering but uniform impedance vs. bottom lit foot with non-uniform impedance values based on MRI density values. (See color plate for full size).*

[Jen01] JENSEN H. W.: *Realistic Image Synthesis using Photon Mapping*. AK Peters, 2001. 3

[JMLH01] JENSEN H. W., MARSCHNER S. R., LEVOY M., HANRAHAN P.: A practical model for subsurface light transport. In *Proceedings of the 28th annual conference on computer graphics and interactive techniques* (2001), ACM Press, pp. 511–518. 1, 2, 3, 5, 6

[Joh70] JOHNSON C. C.: Optical diffusion in blood. In *IEEE Trans.* (1970), pp. 129–133. 4

[Kaj86] KAJIYA J. T.: The rendering equation. In *SIGGRAPH '86* (1986), ACM Press, pp. 143–150. 2

[KD98] KINDLMANN G., DURKIN J. W.: Semi-automatic generation of transfer functions for direct volume rendering. In *IEEE Symposium on Volume Visualization* (1998), pp. 79–86. 6

[KPH*03] KNISS J., PREMOZE S., HANSEN C., SHIRLEY P., MCPHERSON A.: A model for volume lighting and modeling. *IEEE Transactions on Visualization and Computer Graphics 9*, 2 (2003), 150–162. 3

[KPHE02] KNISS J., PREMOZE S., HANSEN C., EBERT D.: Interactive translucent volume rendering and procedural modeling. In *Proceedings of the conference on Visualization '02* (2002), IEEE Computer Society, pp. 109–116. 1, 3

[KV84] KAJIYA J., VON HERZEN B.: Ray tracing volume densities. In *Computer Graphics (SIGGRAPH '84 Proceedings)* (July 1984), Christiansen H., (Ed.), vol. 18, pp. 165–174. 2

[Max94] MAX N. L.: Efficient Light Propagation for Multiple Anisotropic Volume Scattering. In *Fifth Eurographics Workshop on Rendering* (Darmstadt, Germany, 1994), pp. 87–104. 1, 3

[MKB*03] MERTENS T., KAUTZ J., BEKAERT P., SEIDELZ H., VAN REETH F.: Interactive rendering of translucent deformable objects. In *Proceedings of the 14th Eurographics workshop on Rendering* (2003), Eurographics Association, pp. 130–140. 3

[MSM*04] MAX N., SCHUSSMAN G., MIYAZAKI R., IWASAKI K., NISHITA T.: Diffusion and multiple anisotropic scattering for global illumination in clouds. *Journal of WSCG 12*, 3 (2004), 277–284. 3

[PH97] PANFILOV A. V., HOLDEN A. V. (Eds.): *Compu-*

© The Eurographics Association 2005.

tational Biology of the Heart. John Wiley & Sons, 1997. 3

[Pra88] PRAHL S. A.: *Light Transport in Tissue*. PhD thesis, University of Texas at Austin, 1988. 2, 3

[PTVF92] PRESS W. H., TEUKOLSKY S. A., VETTERLING W. T., FLANNERY B. P.: *Numerical Recipes in C*. Press Syndicate of the University of Cambridge, 1992. 5

[REHL03] RILEY K., EBERT D., HANSEN C., LEVIT J.: Visually accurate multi-field weather visualization. In *Proceedings IEEE Visualization* (October 2003), pp. 279–286. 1, 3

[RT87] RUSHMEIER H., TORRANCE K.: The zonal method for calculating light intensities in the presence of a participating medium. *Computer Graphics (SIGGRAPH '87 Proceedings) 21*, 4 (July 1987), 293–302. 2

[Sta95] STAM J.: Multiple scattering as a diffusion process. In *Proceedings of the 6th Eurographics Workshop on Rendering* (Dublin, Ireland, 1995), pp. 51–58. 1, 2, 3

© The Eurographics Association 2005.